# Structures and Spectroscopic Characteristics of 5,6-Dihydro-6-thymyl and 5,6-Dihydro-5-thymyl Radicals by an Integrated Quantum Mechanical Approach Including Electronic, Vibrational, and Solvent Effects

**F. Jolibois,[†] J. Cadet,[†] A. Grand,[†] R. Subra,[‡] N. Rega,[§] and V. Barone*[,§]**

*Contribution from the Département de Recherche Fondamentale sur la Matière Condensée/SCIB/CEA-GRENOBLE 17, Rue des Martyrs F-38054 Grenoble, Cedex 09, France, Laboratoire d'Etudes Dynamiques et Structurales de la Sélectivité (LEDSS), Université Joseph Fourier, 301 Avenue de la Chimie, BP 53X, F-38041 Grenoble, Cedex, France, and Dipartimento di Chimica, Università Federico II, via Mezzocannone 4, I-80134 Napoli, Italy*

*Received July 9, 1997. Revised Manuscript Received November 17, 1997*

**Abstract:** A recently developed quantum mechanical approach devoted to the study of unstable species in solution was applied to isomeric radicals resulting from the addition of hydrogen atoms to thymine. The computational protocol includes either post-Hartree−Fock or density functional electronic computations, together with simulation of the solvent by a polarizable continuum, and averaging of spectroscopic properties over the most important vibrational motions. Concerning electronic computations, hybrid Hartree−Fock/density functional models (here B3LYP) provide reliable results both for structural and spectroscopic parameters. In contrast, pure Hartree−Fock or low-order perturbative many-body approaches (here MP2) stand against considerable difficulties in the treatment of open-shell systems. Starting from B3LYP computations, vibrational averaging by the out of plane motions and, to a lower extent, consideration of solvent effects lead to remarkable agreement between the computed hyperfine coupling constants and experimental data.

## 1. Introduction

Pyrimidine and purine bases are preferential DNA targets for free radical-mediated damage. In the case of thymine H atoms add preferentially to the $C_5-C_6$ bond and the resulting radicals can be further transformed, yielding different stable products with a saturated $C_5-C_6$ bond. Since the characterization of the 5,6-dihydro-5-thymyl radical in irradiated DNA,[1] extensive studies of the radiation-induced radicals of thymine were performed. Among these compounds, the well-known 5,6-dihydro-6-thymyl (referred to as 6-yl) and 5,6-dihydro-5-thymyl (referred to as 5-yl) radicals were the subject of structural investigations during the past decades, mainly using electron paramagnetic resonance (EPR) spectroscopy.[2−7] Both radicals represent key intermediates in the $H^{\bullet}$ addition reaction leading to the formation of thymine lesions such as 5,6-dihydrothymine.[8] In the case of the 5-yl radical, the average hyperfine coupling constant of the hydrogens of the methyl group is well-defined with a value of approximately 20G. On the other hand, inasmuch as the experimental conditions are very different, a wide set of hyperfine coupling constants for the methylene group in position 6 is available. This is illustrated by the fact that the two protons are found equivalent in some investigations,[2,3] whereas, in other studies, the two $\beta$ protons exhibit different hyperfine coupling constants.[4,5] Only a few data are available for the 6-yl radical. In addition, the hyperfine coupling constants of $H^{\alpha}$ and $H^{\beta}$ atoms are not yet unambiguously defined.[6,7] In such a context, a computational study aimed at determining the structures of the two radicals together with the estimation of hyperfine coupling constants should provide valuable information.

Determination of hyperfine coupling constants of free radicals constitutes a severe challenge to theoretical chemistry, since they are related to subtle details of the electronic wave function. This has stimulated much work, and the most sophisticated post Hartree−Fock[9−13] models are providing wave functions of sufficient quality. However, these methods are not suitable for

[†] Matière Condensée/SCIB/CEA-GRENOBLE.
[‡] Université Joseph Fourier.
[§] Università Federico II.

(1) (a) Ehrenberg, A.; Ehrenberg, L.; Löfroth, G. *Nature, London* **1963**, *200*, 376. (b) Salovey, R.; Shulman, R. G.; Walsh, W. M., Jr. *J. Chem. Phys.* **1963**, *30*, 839. (c) Pershan, P. S.; Shulman, R. G.; Wyluda, B. J.; Eisinger, J. *Physics* **1964**, *1*, 163.
(2) Ormerod, M. G. *Int. J. Rad. Biol.* **1965**, *9*, 291−300.
(3) (a) Salovey, R.; Shulman, R. G.; Walsh, W. M. *J. Chem. Phys.* **1963**, *39*, 839−840. (b) Pershan, P. S.; Shulman, R. G.; Wyluda, B. J., Eisinger, J. *Science* **1965**, *148*, 378−380.
(4) Srinivasan, V. T.; Singh, B. B.; Gopal-Ayengar, A. R. *Int. J. Rad. Biol.* **1968**, *15*, 89−93.
(5) (a) Holroyd, R. A.; Glass, J. W. *Int. J. Rad. Biol.* **1968**, *14*, 445−452. (b) Henriksen, T. *Radiat. Res.* **1969**, *40*, 11−25. (c) Henriksen, T.; Jones, W. B. G.. *Radiat. Res.* **1971**, *45*, 420−433.
(6) Henriksen, T.; Snipes, W. *J. Chem. Phys.* **1970**, *52*, 1997−2000.
(7) Henriksen, T.; Snipes, W. *Radiat. Res.* **1970**, *42*, 255−269.
(8) Fuciarelli, A. F.; Wegher, B. J.; Blakely, W. F.; Dizdaroglu, M. *Int. J. Radiat. Biol.* **1990**, *58*, 397.
(9) (a) Sekino, H.; Bartlett, R. J. *J. Chem. Phys.* **1985**, *82*, 4225. (b) Pereira, S. A.; Watts, J. D.; Bartlett, R. J. *J. Chem. Phys.* **1994**, *100*, 1425.
(10) Carmichael, I. *J. Phys. Chem.* **1991**, *95*, 6198.
(11) Feller, D.; Glendening, E. D., McCullough, E. A., Jr.; Miller, R. J. *J. Chem. Phys.* **1993**, *99*, 2829.
(12) Fernandez, B.; Jørgensen, P.; McCullough, E. A., Jr.; Symons, J. *J. Chem. Phys.* **1993**, *99*, 5995.
(13) (a) Engels, B. *J. Chem. Phys.* **1994**, *100*, 1380. (b) Suter, H. U.; Engels, B. *J. Chem. Phys.* **1994**, *100*, 2936.

S0002-7863(97)02284-1 CCC: $15.00 
Published on Web 02/12/1998

systematic studies of large molecules. Recent investigations show that, at least for carbon centered $\pi$ and quasi-$\pi$ radicals, low-order many-body perturbative approaches give spin densities at nuclei that are close to those obtained by more sophisticated methods.[9,14,15] On these grounds, a second-order perturbative treatment based on an unrestricted wave function (UMP2) was selected in the present work. More recently it has been shown by different groups[16,17] that density functional (DF) approaches are very promising also for the study of magnetic properties. Inclusion of some exact exchange in conventional DF models further improves the results, leading these models, in particular the so-called B3LYP method, to reproduce geometric and electronic characteristics of open-shell systems with remarkable accuracy.[18] As a consequence, parallel calculations will be performed at the B3LYP level for all the species at hand.

From another point of view, averaging of the hyperfine coupling constants by large amplitude vibrational motions can sometimes be significant; for instance, the isotropic hyperfine splitting of $^{13}$C in methyl radical is enhanced by about 30% by vibrational averaging.[14b] The combined use of spin densities obtained by either post-HF or B3LYP methods utilizing purposely tailored basis sets and proper account of vibrational modulation effects through effective large amplitude nuclear Hamiltonians[19] was repeatedly shown to provide a powerful and reliable tool to investigate EPR features of flexible radicals.[14,20] More recently, it became possible to take into account the effect of solvent in further modulating magnetic properties. This was achieved through the implementation and validation of refined continuum models in powerful electronic packages.[21−23] The above three ingredients (reliable and fast electronic methods, vibrational averaging and solvent effects) define a general and powerful protocol for the study of unstable species in solution. Here, we apply this general approach to a comprehensive study of the structures and the magnetic properties of 5-yl and 6-yl radicals.

## 2. Methodology

Electronic computations *in vacuo* were performed with the help of the Gaussian-94[24] and Dgauss[25,26] codes. Stationary points for both radicals were located by full geometry optimizations, using quasi-Newton techniques[27] and characterized diagonalizing Hessian matrices computed either analytically or by finite differences of analytical gradients. Hartree−Fock (HF) computations for open-shell systems were performed using both the unrestricted (UHF[28]) and the restricted open-shell (ROHF[29]) formalisms. Starting from UHF wave functions, some electron correlation was introduced by many-body perturbation theory employing the Møller−Plesset Hamiltonian partitioning[30] carried up to second order (UMP2).

Density functional calculations were carried out within the unrestricted Kohn−Sham (UKS) formalism using either the so-called VWN local functional[31] implemented in the Dgauss program (LDA) or the Becke three-parameter functional[32] as modified to include the LYP correlation functional[33] (B3LYP) in the Gaussian-94 program.

On the basis of previous experience,[14,18] the Dunning's [4,2;2] contraction of the Huzinaga (9s,5p;4s) basis[34a] augmented by single polarization functions on all atoms[34b] (hereafter referred to as D95(d,p)) has been our standard for all calculations using the Gaussian-94 program. Improved magnetic properties were obtained at the B3LYP level using the EPR-2 basis set, which was specifically optimized for this purpose.[22,35] In the Dgauss package, a polarized split valence orbital basis set (DZVP)[36] especially optimized for DF computations and a (7/3/3;7/3/3) auxiliary basis set (A1)[37] were used.

Isotropic hyperfine coupling constants $a_N$ are related to the spin densities at the corresponding nuclei by[38]

$$a_N = \frac{8\pi}{3h} g_e \beta_e g_N \beta_N \sum_{\mu,\nu} P_{\mu,\nu}^{\alpha-\beta} \langle \varphi_\mu | \delta(r_{kN}) | \varphi_\nu \rangle$$

where $g_e$ is the free electron g-factor and $h$, the Planck constant. In the present work, all the values are given in Gauss (1 G = 0.1 mT), assuming that the free electron $g$ value is appropriate also for the radicals. To convert data to MHz, one has to multiply them by 2.8025.

The study of large amplitude vibrations requires, especially in the case of relatively large molecules, some separation between the active large amplitude motion (LAM) and the *spectator* small amplitude modes (SAM). In the present work

(14) (a) Barone, V.; Minichino, C.; Faucher, H.; Subra, R.; Grand, A. *Chem. Phys. Lett.* **1993**, *205*, 324. (b) Barone, V.; Minichino, C. Grand, A.; Subra, R. *J. Chem. Phys.* **1993**, *99*, 6787. (c) Barone, V.; Grand, A.; Minichino, C.; Subra, R. *J. Phys. Chem.* **1993**, *97*, 6355.

(15) (a) Cramer, C. J. *J. Am. Chem. Soc.* **1991**, *113*, 2439. (b) Cramer, C. J. *Chem. Phys. Lett.* **1993**, *202*, 297. (c) Cramer, C. J.; Lim, M. H. *J. Phys. Chem.* **1994**, *98*, 5024.

(16) (a) Barone, V.; Adamo, C.; Russo, N. *Chem. Phys. Lett.* **1993**, *212*, 5. (b) Barone, V.; Adamo, C.; Russo, N. *Int. J. Quantum. Chem.* **1994**, *52*, 963. (c) Adamo, C.; Barone, V.; Fortunelli, A. *J. Phys. Chem.* **1994**, *98*, 8648.

(17) (a) Eriksson, L. A.; Malkin, V. G.; Malkina, O. L.; Salahub, D. R.; *J. Chem. Phys.* **1993**, *217*, 24. (b) Kong, J.; Eriksson, L. A.; Boyd, R. J. *Chem. Phys. Lett.* **1993**, *217*, 24. (c) Eriksson, L. A.; Malkina, O. L.; Malkin, V. G.; Salahub, D. R.; *J. Chem. Phys.* **1994**, *100*, 5066. (d) Austen, M. A.; Eriksson, L. A.; Boyd, R. J. *Can. J. Chem.* **1994**, *72*, 695.

(18) (a) Barone, V. *Chem. Phys. Lett.* **1994**, *226*, 392. (b) Barone, V. *J. Chem. Phys.* **1994**, *101*, 6834. (c) Adamo, C.; Barone, V.; Fortunelli, A. *J. Chem. Phys.* **1995**, *102*, 384.

(19) (a) Minichino, C.; Barone, V. *J. Chem. Phys.* **1994**, *100*, 3717, (b) Barone, V.; Minichino, C. *Theochem.* **1995**, *330*, 325.

(20) (a) Barone, V.; Adamo, C.; Grand, A.; Brunel, Y.; Fontecave, M.; Subra. R. *J. Am. Chem. Soc.* **1995**, *117*, 1083. (b) Barone, V.; Adamo, C.; Grand, A.; Jolibois, F.; Brunel, Y.; Subra. R. *J. Am. Chem. Soc.* **1995**, *117*, 12618.

(21) Cossi, M.; Barone, V.; Cammi, R.; Tomasi, J. *Chem. Phys. Lett.* **1996**, *255*, 327.

(22) Rega, N.; Cossi, M.; Barone, V. *J.; Chem. Phys.* **1996**, *105*, 11060.

(23) Barone, V. *Chem. Phys. Lett.* **1996**, *262*, 201.

(24) Frisch, M. J.; Trucks, G. W.; Schlegel, H. B.; Gill, P. M. W.; Johnson, B. G.; Robb, M. A.; Cheeseman, J. R.; Keith, T. A.; Petersson, G. A.; Montgomery, J. A.; Raghavachari, K.; Al-Laham, M. A.; Zakrzewski, V. G.; Ortiz, J. V.; Foresman, J. B.; Cioslowski, J.; Stefanov, B. B.; Nanayakkara, A.; Challacombe, M.; Peng, C. Y.; Ayala, P. Y.; Chen, W.; Wong, M. W.; Andres, J. L.; Replogle, E. S.; Gomperts, R.; Martin, R. L.; Fox, D. J.; Binkley, J. S.; Defrees, D. J.; Baker, J.; Stewart, J. P.; Head-Gordon, M.; Gonzalez, C.; Pople, J. A. GAUSSIAN 94; Gaussian. Inc.: Pittsburgh, PA, 1995.

(25) Andzelm, J.; Wimmer, E. *J. Chem. Phys.* **1992**, *96*, 1280.

(26) UNICHEM 4.0 electronic structure modeling package available from the Oxford Molecular Group

(27) Schlegel, H. B. In J. Wiley & Sons: *Ab initio methods in Quantum Chemistry*; Lawley, K. P., Ed.; 1987; p 249.

(28) Pople, J. A.; Nesbet, R. K. *J. Chem. Phys.* **1959**, *22*, 571.

(29) McWeeny, R.; Dierksen, G. *J. Chem. Phys.* **1968**, *49*, 4852.

(30) Møller, C.; Plesset, M. S. *Phys. Rev.* **1934**, *46*, 618.

(31) Vosko, S.; Wilk, L.; Nursair, M. *Can. J. Phys.* **1980**, *58*, 1200.

(32) Becke, A. D. *J. Chem. Phys.* **1993**, *98*, 5648.

(33) Lee, C.; Yang, W.; Parr, R. G. *Phys. Rev.* **1988**, *B37*, 785.

(34) (a) Dunning, T. H., Jr. *J. Chem. Phys.* **1970**, *53*, 2823. (b) Dunning, T. H., Jr.; Hay, P. J. In *Modern Theoretical Chemistry*; Schaefer, H. F., III, Ed.; Plenum Press: New York, 1977, Vol 2, Chapter 1.

(35) Barone, V. In *Recent Advances in Density Functional Methods. Part 1*; Chong, D. P., Ed.; World Scientific: Publishing: 1996; Chapter 8, p 278.

(36) Andzelm, J. Radzio, E.; Salahub, D. R. *J. Comput Chem.* **1988**, *6*, 520.

(37) Godbout, R.; Salahub, D. R.; Andzelm, J.; Wimmer, E. *Can. J. Chem.* **1992**, *70*, 560;

the LAM is assumed to occur along the linear synchronous path (LSP),[39] which is invariant upon isotopic substitutions and also well defined beyond energy minima. The LSP is obtained through linear variations of all the geometrical parameters between the energy minima taking into the proper consideration the relative orientations of successive structures.[40] Then the path in mass weighted Cartesian cordinates is parametrized in terms of its arc length *s*, referred to as the linear synchronous coordinate (LSC).

When the coupling terms are negligible, the adiabatic Hamiltonian governing the motion along the LSP assumes the simple form[41]

$$H(s,n) = \frac{1}{2}p_f^2 + V_{ad}(s,n)$$

where $^1/_2 p_f^2$ is the kinetic energy operator for the nuclear motion and

$$V_{ad}(s,n) = V_0(s) - V_0(s^0) + \eta\sum_{i=1}^{f-1}\left(n_i + \frac{1}{2}\right)(\omega_i(s) - \omega_i(s^0)$$

the $\omega_i(s)$'s being the harmonic frequencies of small amplitude vibrations as a function of the LSC, and $s^0$ refers to a suitable reference structure lying on the path. If the quantum numbers and the vibrational frequencies of SAM's do not vary along the path, the motion along the LSP is governed by the bare potential $V_0(s)$.

The vibrational states supported by this effective one-dimensional Hamiltonian can be found using the numerical procedure described elsewhere.[42,43] Then, the expectation value $\langle O\rangle_T$ of a given observable at absolute temperature $T$ is given by

$$\langle O\rangle_T = O_{ref} + \frac{\sum_{j=0}^{\infty}\langle j|\Delta O|j\rangle \exp[(\epsilon_0 - \epsilon_j)/KT]}{\sum_{j=0}^{\infty}\exp[(\epsilon_0 - \epsilon_j)/KT]}$$

where $O_{ref}$ is the value of the observable at the reference configuration, $\Delta O(s)$ is the expression (here a spline fit) giving its variation as a function of the progress variable *s*, and $|j\rangle$ is a vibrational eigenstate with eigenvalue $\epsilon_j$. All these computations were performed by the DiNa package.[19,43]

Solvent effects on the magnetic properties of thymine radicals were evaluated with the help of a modified version of the Gaussian-94 package including a new effective implementation of the polarizable continuum model (PCM).[21,44] In this model, powerful numerical techniques are used to solve, in an essentially exact way, the quantum mechanical problem of a molecule immersed in a polarizable continuum with the bulk dielectric constant of the solvent. Although the free energy ($G^{solv}$) of the molecule in solution is written as a sum of electrostatic and nonelectrostatic contributions,[21] only the former terms enter the quantum mechanical Hamiltonian, thus modifying at the same time the energy and the electronic characteristics. The results are, of course, critically dependent on the shape and the dimensions of the cavity created by the solute in the solvent. Here we use the UAHF model that has been recently introduced and validated.[45] Recent studies show that this PCM model coupled with B3LYP Hamiltonian provides reliable results for open-shell species in aqueous solution.[22,23,46]

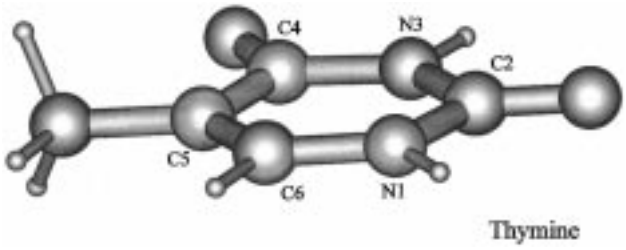


**Figure 1.** Structure and atom labeling of thymine.

**Table 1.** Optimized Geometries of Isolated Thymine

| | B3LYP/D95(d,p) | MP2/D95(d,p) | MP2/6-31G(d)[47] |
|---|---|---|---|
| N1−C2 | 1.390 | 1.387 | 1.386 |
| C2−N3 | 1.388 | 1.389 | 1.386 |
| N3−C4 | 1.409 | 1.406 | 1.403 |
| C4−C5 | 1.473 | 1.468 | 1.462 |
| C5−C6 | 1.357 | 1.361 | 1.354 |
| C2−O2 | 1.223 | 1.228 | 1.225 |
| C4−O4 | 1.226 | 1.233 | 1.230 |
| C5−CMe | 1.504 | 1.501 | 1.496 |
| N3−C4−O4 | 120.3 | 120.6 | 120.7 |
| C2−N3−C4 | 128.1 | 128.5 | 128.6 |
| N1−C2−N3 | 112.7 | 112.5 | 112.2 |
| C6−N1−C2 | 123.8 | 123.9 | 124.1 |
| C5−C6−N1 | 122.7 | 122.4 | 122.4 |
| C4−C5−C6 | 118.0 | 118.2 | 118.4 |
| N3−C4−C5 | 114.6 | 114.4 | 114.4 |
| O2−C2−N3 | 124.1 | 124.0 | 124.2 |
| CMe−C5−C6 | 124.0 | 123.7 | 124.0 |

## 3. Results and Discussion

**3.1. Geometric Structures.** A first investigation was performed on isolated thymine (Figure 1), to check the performances of different methods on a closed-shell system.

Complete geometry optimizations were performed using B3LYP and MP2 methods with the D95(d,p) basis set. The optimized geometrical parameters were compared with MP2/6-31G(d) results obtained in a previous work by Sponer et al.[47] Selected bond lengths and valence and torsion angles are reported in Table 1.

The whole structure remains planar in all cases. The three geometries are similar with averaged differences of 0.003 Å for distances and 0.2° for angles. The latter results confirm that the B3LYP method is efficient and reliable for structural analyses of closed-shell systems.

Next, in the case of open-shell systems, an exhaustive comparison of structural parameters obtained by different computational methods was carried out. Selected bond lengths and valence angles for the 6-yl (Figure 2) and 5-yl (Figure 3) radicals are reported in Table 2 (parts a and b, respectively).

In addition, selected torsion angles are displayed in Table 3.

UHF and ROHF methods give quite similar geometries in both cases. On the other hand, when electronic correlation effects are taken into account (MP2, B3LYP, LDA methods),

(38) Weltner, W., Jr. *Magnetic Atoms and Molecules*; Van Nostrand: New York, 1983.
(39) Halgren, T. A.; Lipscomb, W. N. *Chem. Phys. Lett.* **1977**, *49*, 225.
(40) Zhixing, C. *Theor. Chim. Acta* **1989**, *75*, 481−483.
(41) Miller, W. H.; Handy, N. C.: Adams, J. E. *J. Chem. Phys.* **1980**, *72*, 99−112.
(42) Cremaschi, P. *Mol. Phys.* **1980**, *40*, 401−409.
(43) Barone, V.; Jensen, P.; Minichino, C. *J. Mol. Spectrosc.* **1992**, *154*, 252.
(44) Barone, V.; Cossi, M.; Tomasi, J. *J. Comput. Chem.*, in press.
(45) Barone, V.; Cossi, M.; Tomasi, J. *J. Chem. Phys.* **1997**, 107, 3210.
(46) Rega, N.; Cossi, M.; Barone, V. *J. Am. Chem. Soc.* **1997**, *119*, 12962.
(47) Sponer, J.; Hobza, P. *J. Phys. Chem.* **1994**, *98*, 3161.

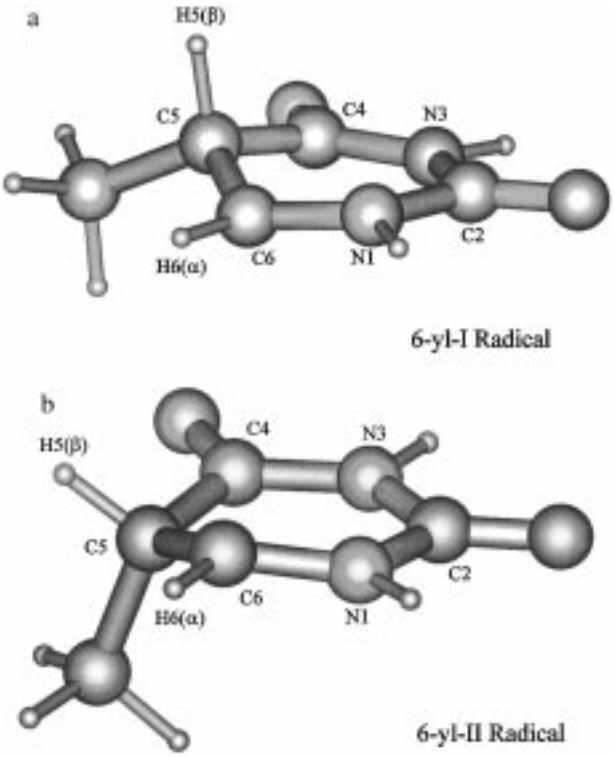


**Figure 2.** Structures of the 6-yl radical obtained at the B3LYP/D95-(d,p) level: (**2a**) 6-yl-I radical and (**2b**) 6-yl-II radical.

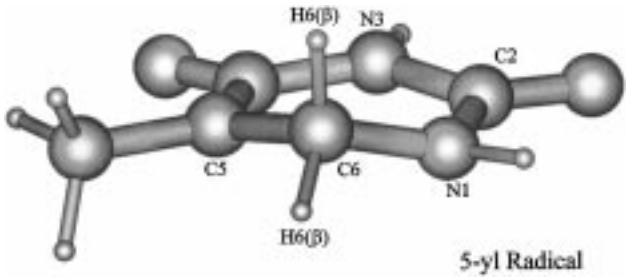


**Figure 3.** Structure of the 5-yl radical obtained at the B3LYP/D95-(d,p) level.

several distortions of the geometry appear. Bond lengths and valence angles are similar, with a maximum difference of 0.025 Å for interatomic distances and 1.5° for angles. However, important modifications of the dihedral angles are observed depending on the method used and on the system studied. For the 6-yl radical, some dihedral angles can be different, more precisely the $C_6-N_1-C_2-N_3$ dihedral angle corresponding to the radical center. Meanwhile, the whole geometry of the six-membered ring adopts an approximately half-chair conformation in all cases. The methyl group has an equatorial orientation, while the $H_5$ hydrogen remains axial. We may note that these conformational features are identical with those found previously in 5,6-dihydrothymine.[48] Since the formation of the 6-yl radical corresponds to the initial step of the reaction leading to the formation of 5,6-dihydrothymine, the conformational features of the product could be already decided in the first reaction step.

The geometry distortions of the 5-yl radical are more significant (see Figure 3 and Table 3). LDA calculations lead to a planar geometry, with $C_5-C_4-N_3-C_2$ and $C_6-N_1-C_2-N_3$ dihedral angles close to zero. On the other hand, B3LYP and MP2 geometry optimizations result in nonplanar structures. Nevertheless, it is interesting to note that the MP2 approach predicts a pyramidality around the $C_5$ and $C_6$ atoms which is significantly larger than that inferred from the B3LYP method. These structures involve different situations for the two hydrogens attached to the $C_6$ carbon atom. In particular, according to LDA computations, the two hydrogen atoms are symmetric with respect to the plane defined by the six-membered ring. However, in the other cases, the ring being no more planar, this symmetry disappears. The latter structural modifications

(48) (a) Konnert, J.; Karel, I. L.; Karle, J. *Acta Crystallogr.* **1970**, *B26*, 770−778. (b) Cadet, J.; Voituriez, L.; Hruska, F. E.; Kan, S. L.; de Leeuw, F. A. A. M.; Altona, C. *Can. J. Chem.* **1985**, *63*, 2861−2868.

**Table 2.** Bond Lengths (in Å) and Valence Angles (in deg) of the Six-membered Ring for 6-yl and 5-yl Radicals

a. 6-yl Radical

| | UHF | ROHF | MP2 | B3LYP | LDA |
|---|---|---|---|---|---|
| N1−C2 | 1.363 | 1.364 | 1.382 | 1.379 | 1.373 |
| C2−N3 | 1.383 | 1.383 | 1.400 | 1.401 | 1.395 |
| N3−C4 | 1.379 | 1.380 | 1.393 | 1.392 | 1.382 |
| C4−C5 | 1.520 | 1.520 | 1.524 | 1.533 | 1.520 |
| C6−N1 | 1.403 | 1.404 | 1.399 | 1.393 | 1.377 |
| O2−C2 | 1.197 | 1.197 | 1.227 | 1.225 | 1.229 |
| O4−C4 | 1.194 | 1.194 | 1.227 | 1.220 | 1.223 |
| CMe−C5 | 1.529 | 1.523 | 1.530 | 1.538 | 1.525 |
| N3−C2−N1 | 114.9 | 114.9 | 113.7 | 113.9 | 113.6 |
| C4−N3−C2 | 128.0 | 127.9 | 128.4 | 128.4 | 128.4 |
| C5−C4−N3 | 115.7 | 115.7 | 114.9 | 115.6 | 115.7 |
| C6−N1−C2 | 122.8 | 122.6 | 123.3 | 124.7 | 124.8 |
| O2−C2−N1 | 123.5 | 123.6 | 123.9 | 123.8 | 123.8 |
| O4−C4−N3 | 120.5 | 120.5 | 120.8 | 120.8 | 120.7 |
| CMe−C5−C4 | 111.6 | 111.6 | 110.9 | 111.2 | 111.6 |

b. 5-yl Radical

| | UHF | ROHF | MP2 | B3LYP | LDA |
|---|---|---|---|---|---|
| N1−C2 | 1.360 | 1.359 | 1.376 | 1.374 | 1.364 |
| C2−N3 | 1.381 | 1.384 | 1.407 | 1.399 | 1.389 |
| N3−C4 | 1.386 | 1.381 | 1.388 | 1.400 | 1.390 |
| C4−C5 | 1.457 | 1.467 | 1.479 | 1.457 | 1.440 |
| C6−N1 | 1.449 | 1.449 | 1.458 | 1.457 | 1.438 |
| O2−C2 | 1.200 | 1.199 | 1.227 | 1.225 | 1.227 |
| O4−C4 | 1.205 | 1.200 | 1.223 | 1.235 | 1.239 |
| CMe−C5 | 1.497 | 1.496 | 1.488 | 1.492 | 1.472 |
| N3−C2−N1 | 115.3 | 115.4 | 114.2 | 114.8 | 115.1 |
| C4−N3−C2 | 126.7 | 127.2 | 127.9 | 127.5 | 127.4 |
| C5−C4−N3 | 115.7 | 115.2 | 113.7 | 115.3 | 115.4 |
| C6−N1−C2 | 124.1 | 124.0 | 122.2 | 125.3 | 126.4 |
| O2−C2−N1 | 123.4 | 123.5 | 124.4 | 123.6 | 123.2 |
| O4−C4−N3 | 120.6 | 120.8 | 121.6 | 120.6 | 120.9 |
| CMe−C5−C4 | 120.9 | 120.3 | 119.7 | 119.9 | 119.0 |

**Table 3.** Selected Dihedral Angles of Thymyl Radicals (in deg)

| | UHF | ROHF | MP2 | B3LYP | LDA |
|---|---|---|---|---|---|
| 6-yl Radical | | | | | |
| C5−C4−N3−C2 | 3.8 | 3.6 | 4.1 | 5.5 | 4.8 |
| H5−C5−C4−N3 | 92.2 | 91.5 | 91.3 | 95.6 | 96.1 |
| CMe−C5−C4−N3 | −150.8 | −151.3 | −151.9 | −149.2 | −149.4 |
| C6−N1−C2−N3 | 11.9 | 12.8 | 9.8 | 4.8 | 3.7 |
| HN3−N3−C2−N1 | −177.5 | −177.7 | −176.3 | −175.8 | −175.6 |
| HN1−N1−C2−N3 | 171.8 | 171.5 | 171.3 | 174.3 | 174.6 |
| 5-yl Radical | | | | | |
| C5−C4−N3−C2 | 12.1 | 10.0 | 13.7 | 8.4 | 2.2 |
| C5Me−C5−C4−N3 | 177.6 | 176.2 | 178.2 | 179.3 | −177.5 |
| C6−N1−C2−N3 | −17.6 | −17.5 | −21.3 | −13.4 | 3.9 |
| H6α−C6−N1−C2 | −89.8 | −89.5 | −82.1 | −98.8 | −123.3 |
| HN3−N3−C2−N1 | −173.8 | −174.8 | −173.3 | −175.3 | −178.8 |
| H6β−C6−N1−C2 | 152.7 | 153.0 | 160.1 | 144.8 | 121.1 |
| HMe1−CMe−C5−C4 | 122.6 | 129.9 | 121.1 | 114.9 | 113.8 |
| HMe2−CMe−C5−C4 | 1.9 | 9.2 | 0.5 | −5.3 | −6.0 |
| HMe3−CMe−C5−C4 | −118.7 | −111.1 | −120.3 | −126.5 | −127.7 |
| HN1−N1−C2−N3 | −172.3 | −172.3 | −169.6 | −173.5 | 179.9 |

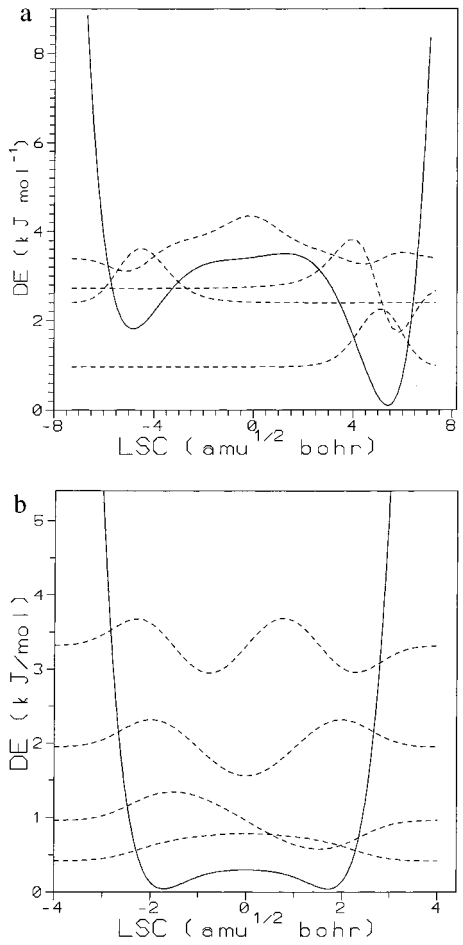


**Figure 4.** (**4a**) Potential energy and lower vibrational wave functions for out of plane motion of $C_5$ atom for 6-yl radical (normalized to 4). (**4b**) Potential energy and lower vibrational wave functions for out of plane motion of $C_6$ for 5-yl radical (normalized to 10).

can have a significant impact on the electronic properties. This mostly concerns EPR hyperfine coupling constants which are particularly sensitive to geometry modifications at, or nearby to, the radical center.[17] While MP2 computations lead to a wrong relative stability of the two radicals,[49] we can expect that the B3LYP model provide reliable data for structural and spin dependent properties.

As mentioned above, different functionals generally give similar conformations for the 6-yl radical. On the other hand, use of the LDA functional leads to a planar conformation for the 5-yl radical, whereas the hybrid B3LYP model suggests a puckered conformation. Starting from this observation, the determination of the energy profile for the inversion of the half-chair structure was studied for the two compounds, at the B3LYP/D95(d,p) level. The corresponding potential curves are given in Figure 4.

In addition, to gain further insights in the role of different conformational features, the anharmonic vibrational levels supported by both potentials were computed using the DiNa[19,43] package. The wave functions corresponding to the lowest vibrational levels of both radicals are shown in Figure 4. The potential curve of the 5-yl radical shows two absolute minima corresponding to the enantiomeric forms of the half-chair conformation (Figure 3). For the 6-yl radical, this curve exhibits also two minima which do not correspond to enantiomeric forms. In one case, the conformation is characterized by the methyl group having an equatorial orientation while the $H_5$ hydrogen remains axial (referred to as 6-yl-I − Figure 2a). The second minimum corresponds to a structure where the methyl group is in axial position and the $H_5$ in equatorial position (referred to as 6-yl-II − Figure 2b). The potential energy barrier separating the two minima is 2.9 kJ mol$^{-1}$ (from 6-yl-I to 6-yl-II), 1.3 kJ mol$^{-1}$ (from 6-yl-II to 6-yl-I) for 6-yl radical, the transition state corresponding to a planar six-membered ring in both cases. This also applies for the 5-yl radical for which the potential energy barrier between the two equivalent minima is 0.3 kJ mol$^{-1}$.

For the 6-yl radical, the 6-yl-I is the most stable conformer and the potential curve corresponds to an asymmetric double-well. The first vibrational levels are localized inside the potential well. It must be noticed that such a small energy barrier between conformers could be significantly affected by either crystal constraints or other environmental effects. As a consequence, complete equilibration between the two energy minima of 6-yl radical can occur or not, depending on the temperature or the origin of the radical.

As the 5-yl radical is concerned, the potential curve corresponds to a "quasi-planar system" with a ground vibrational level located above the potential barrier and peaked at the planar structure. Thus, consideration of vibrational effects leads to an average planar geometry for that radical.

**3.2. E.P.R. Hyperfine Coupling Constants.** During the past decades, a large body of EPR experimental data on the 5-yl and 6-yl radicals became available. While both radicals were studied, the amount of results reported for the 6-yl radical is significantly lower.

**3.2.1. The 6-yl Radical.** EPR hyperfine coupling constants (*hcc*) of the methyl protons are very weak. For the isotropic *hcc* of $H^{\alpha}$ and $H^{\beta}$, two sets of experimental parameters can be found in the literature (Table 4).

The first one concerns the 6-yl radical generated by irradiation of a crystal of 5,6-dihydrothymine at 77 K.[6] The spectrum attributed to this radical has the following assignment: $|a_{H\alpha}| = 17.4$ G and $|a_{H\beta}| = 44.0$ G. The second EPR spectrum was obtained upon irradiation of a crystal of thymine.[7] The assignment of the spectrum led to the following parameters: $|a_{H\alpha}| = 28.3$ G and $|a_{H\beta}| = 17.1$ G. When the radical is formed from 5,6-dihydrothymine, the splitting of the $\beta$-hydrogen is the largest one (44.0 G). In that case, the $C_5-H$ bond seems to be almost perpendicular to the molecular mean plane. On the other hand, when the same radical is generated from thymine, a much lower *hcc* is observed for $H^{\beta}$. Consequently, the $C_5-H$ bond should be closer to the average plane of the molecule in this case. The isotropic value observed for the α-hydrogen by the second experience is significantly larger than the usual splittings observed in alkyl radicals.[50] Henriksen et al.[7] argued that it may be a consequence of a "slight change in the hybridization" of the carbon atom containing the unpaired electron in a $p_{\pi}$ orbital.

As a first step, we decided to evaluate and compare the performances of different methods for the evaluation of *hcc*'s. The most significant results obtained using the D95(d,p) basis set are shown in Table 5.

It is quite apparent that, in the case of the 6-yl radical in its more stable conformation, a too large splitting for the α-hydrogen is inferred from UHF/UHF calculations. In contrast, MP2/MP2 computations lead to a too small splitting for the

(49) Jolibois, F.; Barone, V.; Grand, A.; Subra, R.; Cadet, J., submitted for publication.

(50) Fessenden, R. W.; Schuler, R. H. *J. Chem. Phys.* **1963**, *39*, 2147−2195.

**Table 4.** Experimental Hyperfine Coupling Constants of Both Radicals

| | 6-yl radical | | | | 5-yl radical | | | | | | | |
|---|---|---|---|---|---|---|---|---|---|---|---|---|
| | ref 6 | | ref 7 | | ref 2 | | ref 3 | | ref 4 | | ref 5 | |
| | $H_\alpha$ | $H_\beta$ | $H_\alpha$ | $H_\beta$ | $H_{\beta1}$ | $H_{\beta2}$ | $H_{\beta1}$ | $H_{\beta2}$ | $H_{\beta1}$ | $H_{\beta2}$ | $H_{\beta1}$ | $H_{\beta2}$ |
| hcc (gauss) | 17.4 | 44.0 | 28.3 | 17.1 | 34.5<br>37.5 | 34.5<br>37.5 | 37.7 | 37.7 | 39.0 | 41.0 | 34.1 | 43.1 |

**Table 5.** Hyperfine Coupling Constants in Gauss (Single Point Energy/Optimized Geometry)

| | UHF/ UHF | MP2/ MP2 | B3LYP/ B3LYP | MP2/ B3LYP | B3LYP/ LDA | MP2/ LDA |
|---|---|---|---|---|---|---|
| | | | 6-yl Radical | | | |
| H5($\beta$) | 37.22 | 34.58 | 39.83 | 37.08 | 43.94 | 40.18 |
| H6($\alpha$) | −31.68 | −15.47 | −17.32 | −20.26 | −17.78 | −20.40 |
| HMe | −1.28 | −0.76 | −0.54 | −0.84 | −0.68 | −0.91 |
| HMe | −1.02 | −0.45 | −0.14 | −0.54 | −0.60 | −0.58 |
| HMe | −1.47 | −0.66 | −0.52 | −0.29 | −0.21 | −0.31 |
| | | | 5-yl Radical | | | |
| H6($\beta$1) | 35.27 | 36.04 | 37.96 | 36.44 | 36.46 | 35.56 |
| H6($\beta$2) | 19.15 | 13.88 | 23.38 | 23.52 | 34.67 | 33.79 |
| HMe | 29.04 | 30.89 | 31.96 | 32.88 | 33.09 | 33.08 |
| HMe | 3.15 | −0.43 | 1.15 | 3.80 | 1.06 | −0.30 |
| HMe | 29.14 | 28.07 | 24.98 | 26.19 | 26.32 | 26.05 |

$\alpha$-hydrogen. According to these results and also by considering the energetic stabilities which were investigated in a previous work,[49] only B3LYP calculations appear sufficiently reliable for the contemporary determination of geometric structures and isotropic *hcc*'s. Consequently, all the other results discussed in this section were obtained at either the B3LYP/D95(d,p) or the B3LYP/EPR-2 levels.

Investigation of hyperfine coupling constants was performed on the two different stable 6-yl-I and 6-yl-II structures. Theoretical averaged values of the *hcc* of the hydrogens of the methyl group are around 2 G. If we consider first the results of the irradiation of the 5,6-dihydrothymine crystal, the conformation of the 6-yl radical is characterized by an axial orientation of the $\beta$-hydrogen.[6] Computations performed on the 6-yl-I radical (axial $\beta$-hydrogen) lead to hyperfine coupling constants with an error lower than 2% for the $\alpha$-hydrogen and lower than 9% for the $\beta$-hydrogens with respect to experimental data (Tables 4 and 6a).

On the other hand, if we compare the results obtained for the 6-yl-II radical (equatorial $\beta$-hydrogen) with the experimental data obtained by irradiation of the thymine crystal,[7] the *hcc* calculated for the $\beta$-hydrogen is compatible with the experimental value. It should be noted that the EPR-2 basis set gives a slightly better agreement than the D95(d,p) basis set. Nevertheless, the computed *hcc* for the $\alpha$-hydrogen is about 40% smaller than the experimental data. The theoretical results can be explained by the analysis of the orientation of the $\alpha$-hydrogen which adopts an equatorial orientation with respect to the mean molecular plane, as found for the 6-yl-I radical. Thus, for both structures of the 6-yl radical, the theoretical *hcc* of $H^\alpha$ are similar (17−18 G).

Coming to the vibrational treatment, we recall that, among low-frequency vibrations, only those corresponding to inversion motions involving either the radical center or the atoms nearby this center have a significant effect on EPR parameters. The normal mode which corresponds to C5 inversion is well separated and has a sufficiently low harmonic frequency (62.6 $cm^{-1}$) to require an anharmonic treatment. Figure 5a shows the evolution of hyperfine splittings connected to the out-of-plane displacement of the C5 atom along the LSP described in the methodological section.

It is quite apparent that the splittings of the considered hydrogens are significantly affected by this deformation. From vibrational treatment and temperature averaging, it clearly appears that the experimental hyperfine coupling constants of the 6-yl radical obtained by irradiation of 5,6-dihydrothymine crystal[6] correspond to that of the 6-yl-I radical at 0 K (Table 6a). At this temperature, only the ground vibrational level located in the region of 6-yl-I minimum is occupied (Figure 4a). Thus, the contribution to *hcc* only proceeds from the last conformer. At higher temperatures, the *hcc* value of $H^\beta$ decreases, while that of $H^\alpha$ slightly increases in absolute value (Table 6a). Due to Boltzmann averaging, the contribution of the 6-yl-II conformer to *hcc* values of the 6-yl radical increases with temperature inasmuch as higher vibrational levels are populated. Consequently, the hyperfine coupling constant of the $\beta$- and $\alpha$-hydrogens of the 6-yl-II radical being smaller and larger, respectively than the corresponding *hcc* of the 6-yl I radical, we must observe a decrease of the $H^\beta$ *hcc* and an increase (in absolute value) of the $H^\alpha$ *hcc* of the 6-yl radical. This trend is well supported by the computed vibrationally averaged couplings (Figure 6a and Table 6a).

At this point, the two sets of experimental results can be analyzed as follows:

(i) For the radical obtained by irradiation of the 5,6-dihydrothymine crystal, the experimental *hcc* values are compatible with the vibrationally averaged values, up to 77 K. This corresponds to a preferential 6-yl-I conformation, only the ground vibrational level being occupied significantly. This situation would correspond to a conformation of the radical trapped by crystal constraints.

(ii) For the radical observed upon irradiation of thymine crystals, the experimental value proposed for the $H^\alpha$ *hcc* appears to be abnormally high, when compared to the usual $\alpha$-hydrogen couplings in free radicals,[50] and can only be accounted for by a strong pyramidalization of the radical center. By contrast, if one accepts to reverse the experimental attribution, i.e., 17.1 G for $a_{H\alpha}$ and 28.3 G for $a_{H\beta}$, the couplings are compatible with the values computed at 298 K (Table 6a). In such a hypothesis, the radical could be created either in the 6-yl-I or 6-yl-II conformations and would give an $\alpha$-hydrogen *hcc* of about 18 G and a $\beta$-hydrogen *hcc* of 34 G. Furthermore, if in the crystal the energy difference between the two conformers is somewhat lower than our theoretical result, a value between 15.6 and 33.8 G (Table 6a) for the $H^\beta$ *hcc* would be reasonable.

In conclusion, depending on the mode of formation of the 6-yl radical, one can expect either a large $\beta$-hydrogen coupling or a medium one but never a large $\alpha$-coupling and a "small" $\beta$-coupling.

**3.2.2. The 5-yl Radical.** EPR measurements were performed on different samples including thymine, thymidine, and DNA. The average value of the isotropic *hcc* of methyl hydrogens is near 20G in all the reported studies.[2−5] However, different values of isotropic hyperfine coupling constants for the two $\beta$-hydrogen atoms ($H^{\beta1}$ and $H^{\beta2}$) were observed (Table 4). In some cases,[2,3] both hydrogens are equivalent and $|a_{H\beta}| = 34.5$, 37.7, or 37.5 G. In other cases,[4,5] the two hydrogens are not

**Table 6.** Theoretical Isotropic Hyperfine Splittings (Gauss) for 6-yl and 5-yl Radical

a. 6-yl Radical

| | 6-yl-I | | | 6-yl-II | | | vibrational averaging | | |
|---|---|---|---|---|---|---|---|---|---|
| | *a* D95(d,p) | *a* EPR-2 | *a* EPR-2/PCM | *a* D95(d,p) | *a* EPR-2 | *a* EPR-2/PCM | $\langle a\rangle_{0\ K}$ EPR-2 | $\langle a\rangle_{77\ K}$ EPR 2 | $\langle a\rangle_{298\ K}$ EPR-2 |
| $H^{CH3}$ | weak | weak | weak | weak | weak | weak | weeak | weak | weak |
| $H^{\alpha}$ | −17.3 | −17.2 | −16.4 | −17.6 | −17.6 | −18.2 | −17.4 | −17.5 | −18.4 |
| $H^{\beta}$ | 39.8 | 43.4 | 43.4 | 14.4 | 15.6 | 16.7 | 43.4 | 40.5 | 33.8 |

b. 5-yl Radical

| | ground state | | planar structure | | | vibrational averaging | | |
|---|---|---|---|---|---|---|---|---|
| | *a* D95(d,p) | *a* EPR-2 | *a* D95(d,p) | *a* EPR-2 | *a* EPR-2/PCM | $\langle a\rangle_{0\ K}$ EPR-2 | $\langle a\rangle_{77\ K}$ EPR-2 | $\langle a\rangle_{298\ K}$ EPR-2 |
| $H^{CH3}$ | 19.3 | 21.2 | 19.1 | 21.3 | 21.6 | 21.3 | 21.3 | 21.3 |
| $H^{\beta1}$ | 23.5 | 25.4 | 33.1 | 34.0 | 35.1 | 33.0 | 32.7 | 32.3 |
| $H^{\beta2}$ | 37.9 | 40.0 | 33.1 | 34.0 | 35.1 | 33.0 | 32.7 | 32.3 |

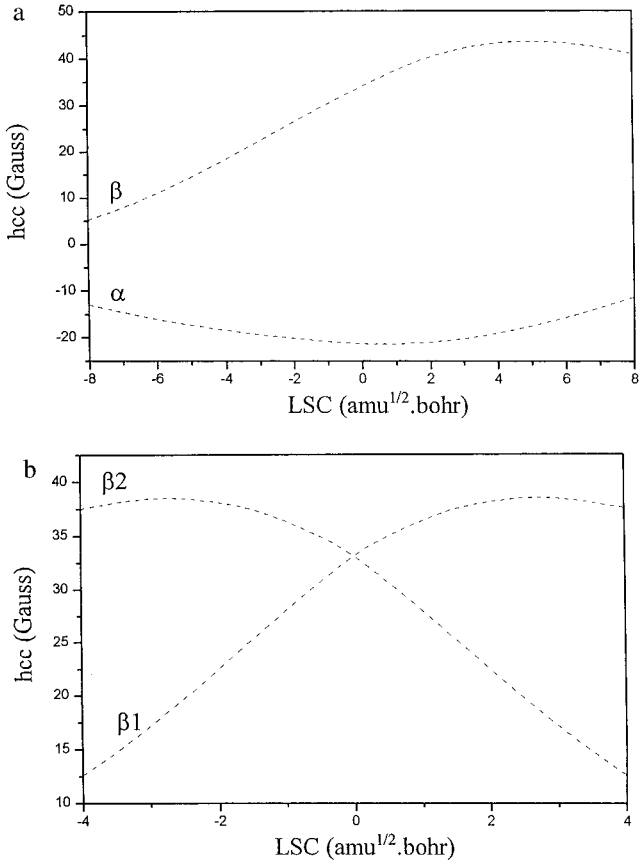


**Figure 5.** Dependence of isotropic *hcc* on the out of plane motion of $C_5$ atom for 6-yl radical (**5a**) and $C_6$ atom for 5-yl radical (**5b**).

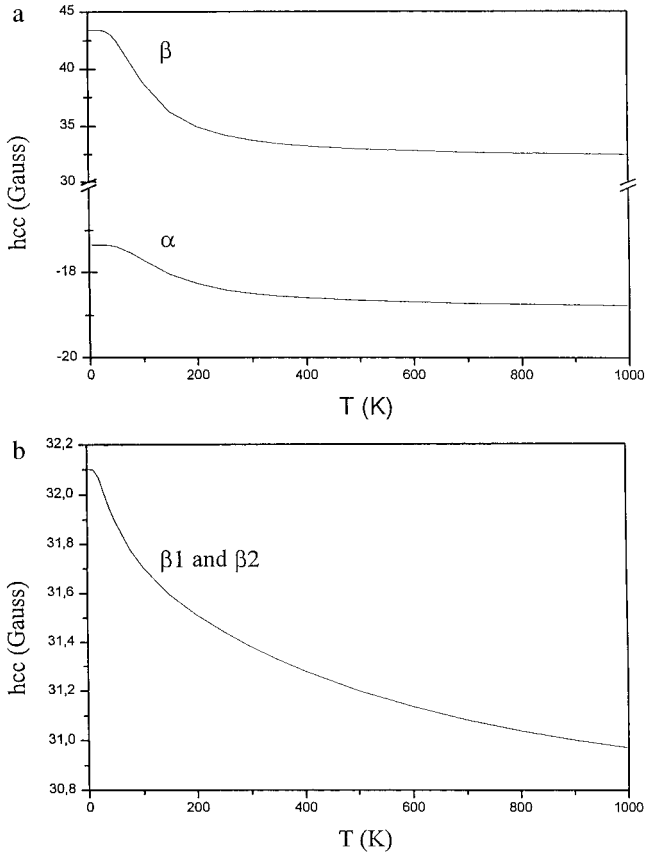


**Figure 6.** Dependence of isotropic *hcc* on temperature for the 6-yl (**6a**) and 5-yl (**6b**) radicals.

equivalent, and the isotropic hcc's values are $|a_{H\beta1}| = 39.0$ or 34.1 G and $|a_{H\beta2}| = 41.0$ or 43.1 G, respectively. It is noteworthy that experimental conditions leading to equivalent and nonequivalent *hcc* exhibit important differences. In particular, either frozen solution or crystal samples are associated with nonequivalent coupling constants. Under these conditions, specific interactions can induce structural constraints which favor a half chair conformation of the pyrimidine cycle. Such conditions are not taken into consideration in our computations, and direct comparison of the resulting theoretical data with experiment may be questionable.

The ground state of the 5-yl radical is characterized by two nonequivalent $\beta$-hydrogens. The theoretical *hcc*'s are the following: $a_{H\beta1} = 23.5$ G and $a_{H\beta2} = 37.9$ G for the D95(d,p) basis set and $a_{H\beta1} = 25.4$ G and $a_{H\beta2} = 40.0$ G for the EPR-2 basis set (Table 6b). While the value of $a_{H\beta2}$ is in good agreement with experimental results, the *hcc* of the other $\beta$-hydrogen is underestimated by about 30%. On the other hand, both hydrogens become equivalent in the planar structure, leading to a single *hcc* value. If we consider the first group of experimental studies giving rise to an *hcc* of 34.5 G for both $\beta$-hydrogens, the differences between theoretical and experimental results are 4% using the D95(d,p) basis set and 1% with the EPR-2 basis set. This value is 2% when PCM model is used to represent the solvent with the EPR-2 basis set (Table 6b). Considering the second set of experimental hcc values (37.5−37.7 G), these differences are more pronounced (D95-(d,p): 12%, EPR-2: 9%, EPR-2/PCM: 6%). Nevertheless, it must be noted that the *hcc* value obtained by including solvent

effects using the PCM model is 1 G larger than the one calculated *in vacuo*. It is also noteworthy that the theoretical average *hcc* of the three hydrogens of the methyl group is not affected by the conformational differences between ground state and planar geometries.

The normal mode which corresponds to C6 inversion is well separated and has a sufficiently low harmonic frequency (69.3 $cm^{-1}$) to require an anharmonic treatment. Figure 5b shows the evolution of hyperfine splittings connected to the out-of-plane displacement of C6 atoms along the LSP described in the methodological section. Starting from the ground-state structure where the two hydrogens of the methylene group are not equivalent, the vibrational treatment leads to identical coupling constants for both $\beta$-hydrogens at 0, 77, and 298 K (Figure 6b and Table 6b). Taking into account that for the equilibrium structure the *hcc*'s are increased by about 1 G when going from (*in vacuo*)/EPR-2 to PCM/EPR-2 computations, our best estimate is 33.4 G. This result involves a maximum error of 10% between theory and the different experimental values.

From these considerations, it is quite evident that the EPR spectrum of the 5,6-dihydro-5-thymyl radical should correspond to that of an effectively planar species with two equivalent $\beta$-hydrogens. Experiments that lead to nonequivalent protons cannot be explained by our theoretical treatment. This can be understood by the fact that the exact experimental conditions were not taken into account by our model.

## 4. Conclusion

In the present study, we have performed a comprehensive analysis of the structure and EPR features of two important radicals derived by addition of hydrogen atom to thymine, namely 5,6-dihydro-5-thymyl and 5,6-dihydro-6-thymyl.

From a methodological point of view, we have further validated a computational protocol associating a hybrid Hartree−Fock/density functional approach to a proper account both of vibrational averaging and of solvent effects.[22,23,35,46] In particular, medium size basis sets are sufficient to reproduce the effect of vibrational averaging and to provide reliable equilibrium values of isotropic coupling constants. Since this kind of computations is routinely feasible for quite large systems, the route seems paved for the fully a priori determination of structural and magnetic properties of radicals of biological interest.

From a more specific point of view, we have unambiguously shown that the 5,6-dihydro-5-thymyl radical is effectively planar, while the 5,6-dihydro-6-thymyl radical adopts an half-chair conformation at low temperature. The planar conformation of the 5-yl radical implies the equivalence of the two $\beta$-hydrogens of the methylene group. Thus, both hydrogens have the same isotropic coupling constant and experimental data which give non equivalent hydrogens cannot be explained. For the 6-yl radical, two nonequivalent energy minima are formed, separated by a low energy barrier. In such a case, temperature effects can be sufficient to modify the values of the $\beta$-hydrogen coupling, giving rise to the values observed experimentally.

**Acknowledgment.** The financial support of the French Ministry of Science and Research (grant ACC-SV N8-MESR, 1995) and of the Italian Research Council (CNR) are gratefully acknowledged.

JA9722842